Hydraulic and mechanical dysfunction of Norway spruce sapwood due to extreme summer drought in Scandinavia

Sabine Rosner[a, *], Notburga Gierlinger[b], Matthias Klepsch[c], Bo Karlsson[d], Rob Evans[e, f], Sven-Olof Lundqvist[g, h], Jan Světlík[i], Isabella Børja[j], Lise Dalsgaard[j], Kjell Andreassen[j], Svein Solberg[j], Steven Jansen[c]

[a] *BOKU Vienna, Institute of Botany, Gregor Mendel Str. 33, A-1180 Vienna, Austria*
[b] *BOKU Vienna, Institute of Biophysics, Muthgasse 11, A-1190 Vienna, Austria*
[c] *Ulm University, Institute of Systematic Botany and Ecology, Albert-Einstein-Allee 11, D-89081 Ulm, Germany*
[d] *The Forestry Research Institute of Sweden (Skogforsk), S-26890 Ekebo, Sweden*
[e] *SilviScan Pty Ltd, 8 Dobell Place, Doncaster East, Victoria 3109, Australia*
[f] *School of Ecosystem and Forest Sciences, University of Melbourne, 500 Yarra Boulevard, Burnley 3121, Victoria, Australia*
[g] *IIC AB, Rosenlundsgatan 48B, SE-118 63 Stockholm, Sweden*
[h] *INNVENTIA AB, now part of RISE, Drottning Kristinas väg 61 B, SE-114 28 Stockholm, Sweden*
[i] *Mendel University in Brno, Centre MendelGlobe – Global Climate Change and Managed Ecosystems, Zemědělská 3, Brno 61300, Czech Republic*
[j] *Norwegian Institute of Bioeconomy Research (NIBIO), P. O. Box 115, NO-1431 Ås, Norway*

ARTICLE INFO

Keywords:
Conduit wall reinforcement
Drought
Global warming
Hydraulic failure
Norway spruce
Picea abies
Structure-function relationships
Wall collapse
Wood cracks

ABSTRACT

Projected climate change scenarios such as frequently occurring dry summer spells are an enormous threat to the health of boreal conifer forests. We identified visible features indicating wood with tracheids predisposed for hydraulic and mechanical dysfunction in Norway spruce, suggest why this is formed during severe summer drought and hypothesised on mechanism that would cause tracheid collapse and stem cracks.

Trees from southern Sweden that showed signs of severe reaction to drought, i.e. stem cracks along the trunk, were compared to healthy, undamaged trees. Rings investigated included those formed in 2006, a year with an extremely dry summer season in the study region. In southern Norway, we investigated trees with and without drought-induced top dieback symptoms. We analysed anatomical features such as tracheid lumen diameter, thickness of cell wall and its various layers (S1, S2 and S3), applied Raman imaging in order to get information on the lignin distribution in the cell wall and the compound middle lamellae and performed hydraulic flow and shrinkage experiments.

Although tracheids in annual rings with signs of collapse had higher tangential lumen diameters than those in "normal" annual rings, we conclude that collapse of tracheid walls depends mainly on wall thickness, which is genetically determined to a large extent. Spruce trees that produce earlywood with extremely thin cell walls can develop wall collapse and internal cracks under the impact of dry spells. We also present a new diagnostic tool for detecting individuals that are prone to cell wall collapse and stem cracks: Lucid bands, i.e. bands in the fresh sapwood with very thin cell walls and inhomogeneous lignin distribution in the S-layers and the compound middle lamellae that lost their hydraulic function due to periods of severe summer drought. The detection of genotypes with lucid bands could be useful for an early selection against individuals that are prone to stem cracks under the impact of severe summer drought, and also for early downgrading of logs prone to cracking during industrial kiln drying.

1. Introduction

Boreal conifer forests play an important role in the national and rural economy of Nordic countries (Schlyter et al., 2006) and provide also important ecosystem services, such as climate regulation by atmospheric carbon fixation (Gauthier et al., 2015; Stinziano et al., 2015; McDowell et al., 2016). Conifer forests of the northern hemisphere can react to warming by increased growth (Kauppi et al., 2016) and some

* Corresponding author.
Email address: sabine.rosner@boku.ac.at (S. Rosner)

https://doi.org/10.1016/j.foreco.2017.11.051
Received 5 October 2017; Received in revised form 20 November 2017; Accepted 24 November 2017
Available online xxx

might still have sufficient resilience to cope with the current temperature increase (Kapeller et al., 2017). Several studies underline however that the prognosticated climate change scenarios (IPCC, 2013) indicate serious threats to the health of boreal conifer forests (Gauthier et al., 2015; Allen et al., 2015; McDowell et al., 2016). High vulnerability is especially expected for species such as Norway spruce (*Picea abies* L. Karst.), in particular when it is grown at the margins of its natural range or cultivated outside its realized niche (Seidl et al., 2017). Norway spruce is an autochthonous species of the alpine timberline (Mayr et al., 2003; Mayr et al., 2014) and of high latitude northern regions (Solberg, 2004; Andreassen et al., 2006; Kapeller et al., 2017), but it has also been widely planted in low elevation regions of Central Europe where increased vulnerability to climate change is expected (Seidl et al., 2017), in particular if summer precipitation would continuously decrease (Spinoni et al., 2017). In that regard, Norway spruce forests planted at the margins of its natural range become increasingly endangered; first hints into this direction are reports of tree mortality after summer droughts in southern Norway (Solberg, 2004; Hentschel et al., 2014; Rosner et al., 2016b), representing the most southern distribution of European high latitude Norway spruce forests (Caudullo et al., 2016).

In general, conifer species have quite high hydraulic safety margins compared to angiosperms; conifer's P_{50}, i.e., the water potential causing 50% conductivity loss, were found to be much lower than minimum water potentials measured on a seasonal basis (Choat et al., 2012). However, conifers are also vulnerable to high conductivity losses because they are supposed to have little capacity to restore a hydraulically functional state after severe summer droughts (McDowell et al., 2008; McDowell, 2011; Meinzer and McCulloh, 2013; Zwieniecki and Secchi, 2015). High hydraulic safety in conifers is achieved by structural modifications in pit membrane design (torus overlap; i.e. the ratio of torus to pit aperture diameter), cell wall thickness and lumen diameters of the tracheids (Bouche et al., 2014). The conduit wall reinforcement ($(t/b)^2$), defined as the second power of the double wall (t) to lumen (b) ratio, was introduced by Hacke et al. (2001) as a proxy for P_{50}. A first prerequisite for high hydraulic safety is a safe cell design with smaller lumen and/or thicker walls in order to resist implosion when the mechanical stresses increase with increasing negative xylem water potential prior to embolism. $(t/b)^2$ proved as a good predictor for P_{50} in empirical studies performed within- (Rosner et al., 2016b) and across conifer species (Bouche et al., 2014). As these risks are highest in earlywood, tracheid dimensions for calculation of t/b have been assessed either in the first tangential files of earlywood (Rosner et al., 2009), in the whole earlywood (Bouche et al., 2014, Rosner et al., 2016a), or along the whole radial file across an annual ring, excluding tracheids that show high deviation from a calculated hydraulic diameter (Mayr and Cochard, 2003; Domec et al., 2009; Hacke and Jansen, 2009; Hereş et al., 2014). Recently, Rosner et al. (2016b) found that $(t/b)^2$ calculated from tangential lumen diameters was more strongly related to P_{50} than $(t/b)^2$ based on the mean- or radial lumen diameter.

Generally, embolism of conifer tracheids is suggested to occur long before walls of normal cells would implode (Bouche et al., 2014). In *Pinus radiata*, collapse was found under the impact of extreme drought stress in poorly lignified tracheids of young trees grown in lysimeters (Barnett, 1976), due to suppression of 4-coumarate-coenzyme A ligase (Wagner et al., 2009), and in deformed trees that had copper deficiency (Downes and Turvey, 1990). Glerum (1970) observed drought rings with signs of collapse in *Picea glauca* seedlings exposed to artificially induced severe drought. Reversible collapse has been reported in (transfusion) tracheids of conifer needles (Cochard et al., 2004; Brodribb and Holbrook, 2005; Zhang et al., 2014). In angiosperms, collapse in xylem of vascular bundles has been found in mutants of *Arabidopsis* (Turner and Somerville, 1997; Carpita and McCann, 2015), in xylem vessels of maize (Kaufmann et al., 2009), in conductive elements of leaf veins of red oak (Zhang et al., 2016) and in sapwood of transgenic poplars (Kitin et al., 2010). Sudden imbalances in free water when trees are hit by lightning may also lead to a sudden tracheid wall collapse (Wimmer, 2002).

In the present study, we focus on signs of extreme reaction to sudden dry summer spells in the wood of Norway spruce trees grown in southern Scandinavia. Although tracheid collapse has only been observed after extreme, often artificially induced, climate conditions, or in mutants, the question arises if this phenomenon will become a problem in the near future under the impact of more frequent, intensive drought spells. Another phenomenon associated with extreme summer drought are cracks which can run for up to several meters along a tree trunk and cause severe economic losses (Caspari and Sachsse, 1990; Persson, 1994; Ferenczy and Tomiczek, 1996). Internal cracking in living trees is suggested to develop in low density wood (Grabner et al., 2006); such wood might also be prone to cell wall collapse. The aims of this study were (a) to investigate tracheid collapse in Norway spruce wood and (b) to increase our understanding of the anatomical predisposition and mechanisms behind tracheid collapse. We screened annual rings of ten trees that showed signs of severe reaction to drought stress, i.e. stem cracks along the trunk, and 64 healthy undamaged trees from three sites in southern Sweden. Annual rings from one site included those formed in 2006, a year with the hottest July in Lund (southern Sweden) since recording started in 1859 (SMHI). In southern Norway, we investigated 110 trees with symptoms of top dieback (induced by drought) and 110 healthy looking trees grown on eleven different sites. Annual rings of 242 trees were scanned for abnormities such as collapsed cell walls or density variations. "Normal" wood and wood with collapsed cells were compared by qualitative and quantitative anatomical investigations on the tissue- (X-ray wood density, scanning electron microscopy (SEM)), the tracheid- (maceration, light microscopy, SilviScan (Evans 1994, 1999)) and cell wall level (transmission electron microscopy (TEM), Raman imaging). Differences in the physiological functioning of wood without- and with signs of collapse were tested by hydraulic flow- and shrinkage experiments. We hypothesize that (a) wall collapse occurs in trees that showed stem cracks, (b) that the thickness of tracheid walls rather than the lumen diameter is the main anatomical character associated with tracheid collapse, and (c) that the collapse causes irreversible mechanical and hydraulic dysfunction of the sapwood. In order to test our hypotheses we performed anatomical investigations on the tissue-, tracheid-, and cell wall level and carried out hydraulic experiments.

2. Material and methods

2.1. Plant material

An overview on the tree sample sets is given in Supplement Table 1 and Supplement Fig. 1. The study is based on plant material from a series of samplings of Norway spruce trees in southern Sweden and southern Norway, including also wood specimens from earlier studies (Rosner et al., 2008, Rosner et al., 2016b).

From an existing sample set (Rosner et al., 2008), specimens from 52 healthy Norway spruce trees were available for additional anatomical analyses (SET 1, Supplement Table 1, Supplement Fig. 1). The sample set comprised six clones growing at two sites in southern Sweden with different water availability (Tönnersjehöden and Vissefjärda). SilviScan technology was applied on 95 sapwood specimens from these trees in order to investigate genetic and site predisposition of cell wall thickness.

In June 2008, 22 Norway spruce trees were selected from a clone archive in Ekebo, located in southern Sweden (SET 2a and SET 2b, Supplement Table 1, Supplement Fig. 1). We selected ten Norway spruce clones with visible cracks along the trunk (Fig. 1a) and ten

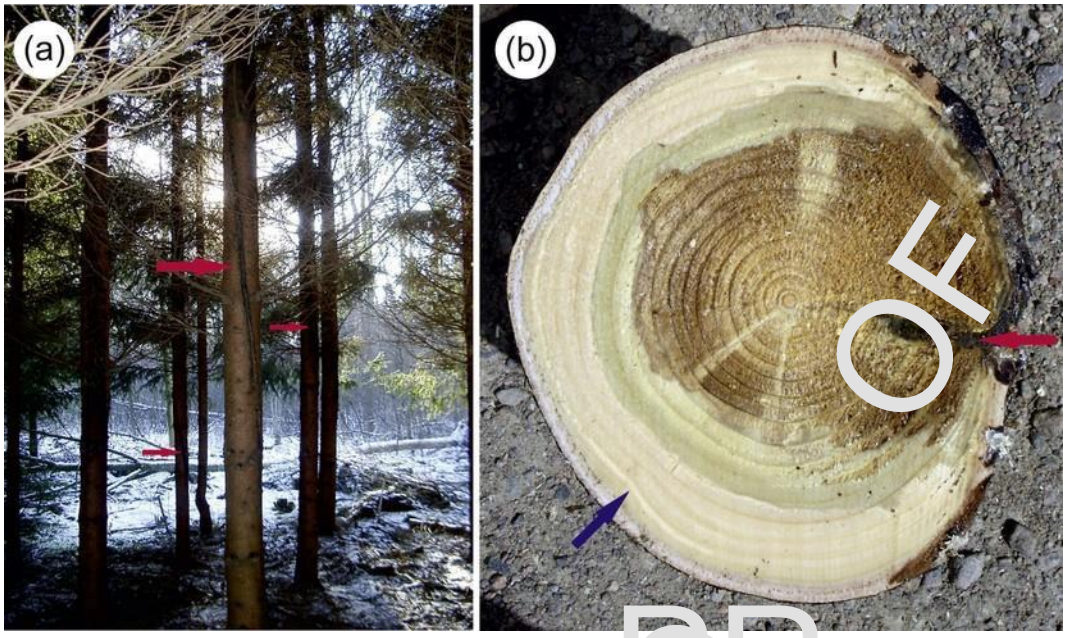

Fig. 1. Norway spruce clones prone to stem cracking. Cracks (indicated by red arrows) can develop several meters along the main trunk (a); after the development of a crack, trees are often invested by fungi (b). A lucid band within the conducting sapwood is indicated by a blue arrow in image (b); the band does not run continuously around the whole perimeter. (For interpretation of the references to colour in this figure legend, the reader is referred to the web version of this article.)

healthy, undamaged, clones. Most of the clones (73%) with visible cracks were infested by pathogenic wood destroying fungi such as *Stereum sanguinolentum* or *Heterobasidion* spp. (Ferenczy and Tomiczek, 1996) and apparently only the outermost annual rings were capable of conducting water (Fig. 1b). In Fig. 1b an extreme example is shown. The sample set (SET 2a, Supplement Fig. 1) comprised also two younger trees (age = 15 years), one clone non-susceptible to stem cracking and one susceptible clone, which showed nevertheless no signs of cracking at the time of harvesting. In total, eleven clones susceptible- and eleven clones not susceptible to stem cracking were selected at Ekebo site.

Trees from southern Norway came from eleven different sites. We investigated in total 220 trees at a field age of 30–70 years (SET 3a and SET 3b, Supplement Table 1, Supplement Fig. 1). Within an area of 250 m^2, ten trees with symptoms of top dieback and the nearest healthy looking neighbour with a quite similar size were selected. From two of the sites, Sande and Hoxmark (SET 3a), not only wood cores were taken, but 24 trees were harvested in September 2011 (Rosner et al., 2016b).

2.2. Sampling

From trees harvested at Ekebo, southern Sweden (SET 2a and SET 2b, n= 22, Supplement Table 1), wood discs were sawn at breast height (1.3 m above the soil). Two wood cores (12 mm in diameter) per tree were taken at breast height of 20 individuals from each of the eleven sites selected in southern Norway (SET 3a and SET 3b, n= 220, Supplement Table 1). In addition, at Sande and Hoxmark, 30 mm thick wood discs were taken from the living crown of felled trees (n= 24, part of SET 3a). Directly after harvesting or coring, all sapwood specimens were transported to BOKU, Vienna, in plastic bags containing some fresh water and 0.01 vol% Micropur (Katadyn Products Inc.). Specimens were stored at −18 °C. Sapwood samples obtained from felled trees at Ekebo were directly after harvesting in the field examined with the naked eye for abnormalities such as bands with a lighter colour than the adjacent sapwood colour (Figs. 1b and a).

Sampling of the sapwood specimens (Supplement Table 1, SET 1) from the Tönnersjehöden and Vissefjärda sites is described in Rosner et al. (2008); in the present study we analysed 95 sapwood beams originating from 52 trees.

Care was taken that none of the wood specimens used in this study contained any reaction wood or traumatic tissue.

2.3. Sapwood hydraulic staining experiments of specimens with lucid bands

Hydraulic staining experiments were performed in July 2008 on defrosted, never dried, sapwood samples from young healthy trees harvested in Ekebo, southern Sweden. Freeze-storage for some weeks has no impact on hydraulic conductivity or vulnerability of Norway spruce sapwood (Mayr et al., 2003; Rosner et al., 2006). Wood specimens (6 mm (radial) × 6 mm (tangential) × 100 mm (longitudinal)) produced with a chisel were fully saturated under low vacuum (Hietz et al., 2008), focusing on samples containing one complete annual ring with wood that had a band of lighter (almost white) colour than the surrounding earlywood of the adjacent rings, hereafter termed “lucid band” (Supplement Fig. 2, Fig. 2a). Flow experiments were performed with 1% solution (w/v) Phloxine-B ((Sigma Chemical Co., St. Louis, MO, USA)) under a hydraulic pressure head of 80 cm, i.e. 8 kPa, (Hietz et al., 2008).

2.4. Wood shrinkage during dehydration of normal wood and wood with lucid bands

Experiments were performed on defrosted, never dried, sapwood samples originating from two young healthy trees harvested in Ekebo, southern Sweden. Wood shrinkage measurements were performed as described in Rosner et al., (2009). Radial wood shrinkage was as- sessed by a load cell (DMS, Type 8416–5500, range 0–500 N; ampli- fication with an inline amplifier for DMS, Type 9235; Burster, Gerns- bach, Germany). Sensors were positioned on the tangential face of fully saturated small sapwood beams (6 mm tangential, 6 mm radial and 100 mm longitudinal) using an acrylic resin clamp assemblage. The whole clamp assemblage was positioned on a balance (resolution

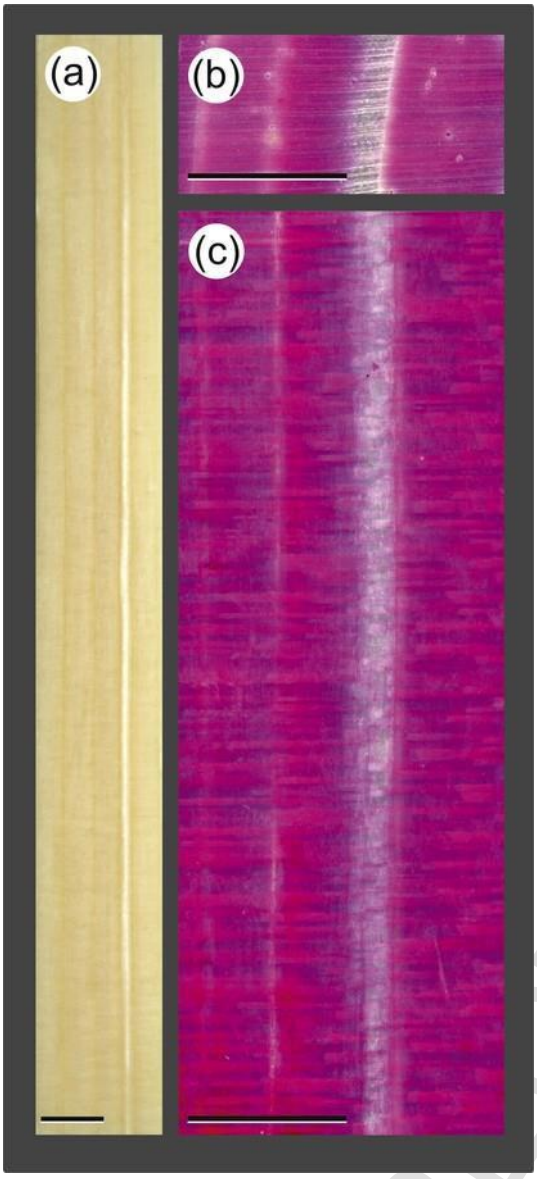

Fig. 2. Phloxine B staining experiment of a lucid band (LB) in Norway spruce sapwood (annual ring 2006) from Ekebo (southern Sweden). In the never dried and fully saturated state, the LB regions have a lighter, almost white, colour compared to the surrounding wood (a); LB remain unstained when flow experiments with the Phloxine B solution are performed. The transverse view is shown in (b), the radial longitudinal view in (a) and (c), reference bars= 3 mm.

10^{-3} g, Sartorius, Göttingen, Germany). Absolute shrinkage was calculated by relating the total radial shrinkage (digital gauge, accuracy 1 µm, Mitutoyo Corporation, Japan) to the total coupling pressure decrease. Dry mass of the wood beams was obtained by drying at 103 °C to constant weight to calculate the relative water loss. Cumulative radial shrinkage was referenced to the nearest 5% relative moisture loss steps.

2.5. Observations at the tissue level: Screening for abnormities and tracheid dimensions

Sapwood samples from the felled trees in southern Norway (specimens from the living crown) and from Ekebo were sawn from the wood discs after thawing in tap water and were kept wet during all preparation steps.

For scanning electron microscopy (SEM), sapwood specimens from SET 2a and two tress of SET 2b (Supplement Table 1, Supplement Fig. 1), were dehydrated in 99% ethanol and dried at ambient temperature. Specimens were mounted on aluminium stubs and were coated with gold using a sputtering device (FL-9496, Balzers Union, Lichtenstein) for 2 min at 13.3 mPa and 40 mA. SEM Observations were carried out with a scanning electron microscope DSM 942 (Carl Zeiss, Oberkochen, Germany) under 9 kV.

For light microscopy, microtome sections with a thickness of 20 µm were produced on a sliding microtome (Jung-Reichert, Vienna, Austria) from all wood cores and sapwood samples of SET 2a, SET 2b, SET 3a and SET 3b (Supplement Table 1, Supplement Fig. 1). Sections of trunk wood specimen from the felled trees (SET 2a, SET 2b and 24 trees of SET 3a) were thereafter stained with methylene blue, dehydrated, and mounted in Euparal (Carl Roth GmbH + Co. KG, Karlsruhe, Germany). Annual rings of the permanent and non-permanent wood sections of in total 242 trees were screened for visual signs of cell wall collapse. In trees from Southern Norway (n = 220, SET 3a and SET 3b) we could investigate annual rings 1980–2011 at breast height as well as rings 2000–2011 from the living crown (n = 24) and in trees from Ekebo, southern Sweden (n = 22), annual rings 2003–2007 at breast height (SET 2a and SET 2b). Cell wall thickness (t) of the radial (t_r) and the tangential cell wall (t_t) and the radial (b_r) and the tangential lumen di- ameter (b_t) were measured in annual rings formed in 2010 in the liv- ing crown of 24 trees from southern Norway (Sande and Hoxmark) and in breast height annual rings 2003–2006 in 22 trees from Ekebo. Cell wall and tracheid dimensions were assessed by means of Image J soft- ware (Schneider et al., 2012) in the first seven radial cell files. In addi- tion, we measured these traits in selected annual rings at breast height of five trees from Norway (n = 3) and Ekebo, Sweden (n = 2); these ad- ditional measurements were only performed for the regions of annual rings where collapsed cells were found. We calculated the conduit wall reinforcement (Hacke et al., 2001) in the radial direction ($(t_r/b_r)^2$) from the square of the radial double cell wall thickness (t_r) and the radial lumen diameter (b_r), and the conduit wall reinforcement in the tangen- tial direction ($(t_t/b_t)^2$) from the square of the tangential double cell wall thickness (t_t) and the tangential lumen diameter (b_t).

From dried small wood beams (Supplement Table 1, SET 1, n= 95 specimens) of 52 treesfrom Tönnersjehöden and Vissefjärda(Sweden) that were used for hydraulic testing in a previous study (Rosner et al., 2008), small wood cubes with radial, tangential and longitudinal dimensions of 6 mm were sawn. Wood specimens from Ekebo (Sweden, SET 2a, n= 2 trees, Supplement Table 1, Supplement Fig. 1), Sandeand Hoxmark (Norway, Supplement Table 1, SET 3a, n= 40 trees) weredefrosted, dehydrated in 99% ethanol and dried at ambient temperature. Thereafter, strips with longitudinal dimension of 7 mm and tangential dimension of 2 mm were produced with a twin-blade saw. Wood strips were then analysed by SilviScan at CSIRO (Australia) and at Innventia (Sweden) (Evans, 1994, 1999). SilviScan is an instrument for efficient measurement of wood and fibre properties, such as wood density, wood stiffness, fibre dimensions and microfibril angle. For the present study, X-ray microdensity, radial and tangential tracheid diameters and cell wall thickness were assessed as averages for consecutive 50 µm radial intervals. After cross-dating the wood cores, a dataset of ring widths (RW) and potential functional traits for each annual ring was calculated. We then defined conduit wall reinforcement in the radial and tangential directions according to above (Rosner et al., 2016b).

2.6. Observations at the tracheid level: maceration of earlywood

About 2 mm thick radial wood sections were prepared with a razorblade from defrosted earlywood of two young trees (age=15) har-

vested in Ekebo (Supplement Table 1, SET 2a) and macerated using Jeffrey's solution (Jeffrey, 1917). Tracheids were thereafter stained with methylene blue, dehydrated and embedded in Euparal (Carl Roth GmbH+Co. KG, Karlsruhe, Germany). Digitization was done with a Leica DM4000 M microscope equipped with a Leica DFC320 R2 digital camera and Leica IM 500 Image Manager image analyzing software (Leica, Wetzlar, Germany).

2.7. Observations at the cell wall level

Observations at the cell wall level were done on four trees from sample SET 2a and SET 2b (Supplement Table 1, Supplement Fig. 1).

Frozen sapwood specimens were thawed in deionised water, dehydrated in ethanol and embedded in Technovit® 7100 (Heraeus Kulzer GmbH, Wehrheim, Germany), which is a plastic embedding system based on 2-hydroxyethyl methacrylate. Transverse semi-thin (1–2μm) sections were made with a Leica RM2235 Manual Rotary Microtome (Leica Biosystems GmbH, Nussloch, Germany). Sections were stained with toluidine blue, crystal violet, or astra-blue/safranine and mounted in Euparal (Carl Roth GmbH+Co. KG, Karlsruhe, Germany). The Technovit® 7100 embedding method has been used in a recent study (Mayr et al., 2014) in order to "conserve" the functional state of bordered pits in Norway spruce. To avoid pit aspiration due to dehydration, it is important to transfer the fully saturated specimen directly into 100% ethanol (Liese and Bauch, 1967).

TEM observations were made on five sapwood specimens per tree. Frozen samples were thawed in deionised water. Specimens were thereafter dehydrated through a graded ethanol series. The ethanol was then gradually replaced with epoxy resin (Sigma-Aldrich Co. LLC, St. Louis, Missouri, USA). Embedded samples were sectioned on an ultra-microtome (Ultracut, Reichert-Jung, Austria). Semi-thin sections were cut with a glass knife (Leica, Nussloch, Germany). Sections were stained with toluidine blue and/or crystal violet, dehydrated and mounted in Euparal. Ultra-thin (60–90 nm) transverse sections were produced with a diamond knife, then attached to Formvar (Agar Scientific, Stansted, UK) and 100 mesh copper grids, and thereafter post-stained with uranyl acetate (Merck, Darmstadt, Germany) and lead citrate (Plano GmbH, Wetzlar, Germany). Observations were carried out with a JEOL JEM-1210 TEM (Jeol, Tokyo, Japan) at 80 kV accelerating voltage.

A confocal Raman microscope (Alpha300, WITec, Germany) equipped with a piezo scanner and a linear polarized NdYag laser (excitation wavelength = 532 nm) was used for high resolution Raman Imaging. The laser light was focused and collected with a diffraction limited spot size through an oil immersion objective (Nikon, 100×, N.A=1.4), guided through a 50μm multimode fibre to a spectrograph (WITec UHTS 300 spectrometer) and detected by a CCD camera (Andor, DV401-BV, 352). Mapping was done on different positions of 2 μm thick in Technovit 7100 embedded sections as well as on 20 μm thick native micro-sections of normal and collapsed tracheids (Supplement Table 1). One spectrum was collected every 0.25 μm with an acquisition time of 0.3 s per spectrum/pixel. From this multi-spectra file, images were computed by integrating over certain ranges of Raman shifts using the ScanCtrlSpectroscopyPlus software (Witec, Germany) and the lignin distribution is shown based on the integration of the aromatic ring stretching vibration at 1600 cm^{-1} (Gierlinger et al., 2012).

2.8. Theoretical implosion pressure

The implosion pressure, i.e. the critical pressure difference between adjacent tracheids that would cause tracheids to implode was calcu- lated from data derived with Image J software from SEM and light microscopy digital images as described in Hacke et al. (2004) and Domec et al. (2009) as (Eq. (1)):

$$P_{\mathrm{impl}} \approx 304 * (1 - D_{\mathrm{a}}/D_{\mathrm{m}}) * (t_{\mathrm{r}}/b_{\mathrm{r}})^2 \quad (1)$$

where D_a is the pit aperture diameter and D_m the pit (membrane) diameter. D_a/D_m was calculated from 20 single measurements for each sample set. We used the simplified formula excluding the quantification of the spacing of the pit apertures distance between pits or between pits and the edge of tracheids for calculating the "ligament efficiency", which quantifies the spacing of the pit apertures in the wall, because the spacing between bordered pits in the radial cell walls was highly variable (Supplement Fig. 2) and calculating a mean value would have obscured the result for P_{impl}. The ligament efficiency was calculated as $\approx 1 - D_a/D_m$. The constant (≈304) is calculated from the strength of the wall material taken as 80 MPa divided by the ratio of b to the tracheid length that was taken as 0.25. The quotient was multiplied by the moment ratio (I_h/I_s), i.e. the ratio of the second moment of area of a tracheid wall with pit chambers (I_h) to that of a solid wall with no pit chambers (I_s) that averages about 0.95 in conifers (Hacke et al., 2004).

2.9. Statistical analyses

Statistical analyses were carried out with SPSS® 21.0. Data in the flow text are given as mean ± standard error (SE). Mean values were ex- amined for significant differences by the Student's *t*-test after testing for normal distribution with the Kolmogorov-Smirnov test. Significant dif- ferences for clones, sites and their interaction were tested using factorial ANOVA. Clones and sites were assumed to be fixed effects in the gen- eral linear models. Correlations between traits and differences in mean values were accepted as significant if P was <0.05.

3. Results

3.1. Macroscopic description of lucid bands

Light coloured, even white bands, hereafter termed "lucid band" (LB), were observed in sapwood specimens from freshly harvested Norway spruce trees in Ekebo, southern Sweden (Fig. 1b, Supplement Fig. 2a and c, Fig. 2a). LBs were found in the first formed earlywood re- gions of the 2006 annual ring (Supplement Fig. 2c), including the part of the 2006 ring perimeter which was not deteriorated by rot at a crack (Fig. 1b). LBs are visible on fresh wood, but can still be detected sev- eral years after sampling if the sapwood is stored frozen directly after harvesting and thereafter thawed in fresh water. However, once the sapwood is dried, these bands show the same colour as the earlywood of adjacent annual rings (Supplement Fig. 2b). LBs were found in trees prone to cracking solely – in two out of eleven individuals. One of these trees was younger and had no crack at the time of harvesting. Artefacts due to dehydration or mechanical damaged that would cause LB can be excluded because (a) stem segments were directly sawn (neither cut nor cored) from the main trunk directly after harvesting and (b) put immediately in water. Only sapwood samples of trees felled at Ekebo site were macroscopically examined directly after harvesting, we therefore cannot provide detailed statistics on the occurrence of LB for the other sites.

3.2. Hydraulic xylem dysfunction in lucid bands

Hydraulic staining experiments showed that the sapwood in LB regions was not hydraulically functional. They remained unstained with Phloxine B (Fig. 2b and c), as no water was transported within these regions. After staining, LB had a light colour, whereas regions that were still capable of conducting water were stained bright magenta.

3.3. Shrinkage in sapwood with and without LB

Radial sapwood shrinkage had a quite different pattern in samples from a young tree where LB regions were found as compared to "normal" wood samples from a tree with the same age. The difference in cumulative shrinkage between the specimens was significant after 20% relative moisture loss (Fig. 3). The maximum radial shrinkage was significantly ($P < 0.01$) higher in specimens that had LB regions ($-3.93 \pm 0.29\%$, $n = 8$) than in "normal" wood ($-2.72 \pm 0.13\%$, $n = 7$).

3.4. Qualitative anatomy of LB at the tissue, tracheid and cell wall level

In regions with LB, tracheids had a more wavy shape (Supplement Fig. 3c and d) compared to tracheids in "normal" sapwood (Supplement Fig. 3a and b). Tracheids in LB (Fig. 4a) were also shorter than tracheids in "normal" wood (Fig. 4b). We assessed a mean tracheid length of 3.62 ± 0.08 mm ($n = 20$) in "normal" earlywood and a length of 2.97 ± 0.10 mm ($n = 20$) for tracheids in the LB regions ($P < 0.001$). Light microscopy observations of LB regions indicated that many tracheids had mechanical deformations (Figs. 5 and 6). Such deformations, hereafter termed "collapse", were found in 9.1% (two clones) of 22 trees harvested in Ekebo, southern Sweden. Signs of collapse were only found in individuals that were prone to stem cracking. In the same individuals, LBs were present. 6.4% (14 trees) of 220 trees investigated in southern Norway had signs of collapsed tracheids too. In tracheids of LB bordered pits were often aspirated (Supplement Fig. 4); an indication that the sapwood in these regions does not contribute to water transport (Fig. 2).

The contents of lignin in cell walls of tracheids with signs of collapse and the thin compound middle lamella (CML) in between them is indicated by red staining with safranin/astra-blue dye (Supplement Fig. 5). The lignin distribution was also visualised with the help of Raman imaging(Fig.7).Whilethe"normal" tracheidsshowedatypicalstraight and thin CMLwithhigh lignin content(whiteareas), the CML in the LB tracheids looks thinner and lesshomogenous. Also within the S layer of LB tracheids a less homogenous lignin distribution was observed than in "normal" earlywood tracheids as indicated by darker regions (lower amount) especially near the cell corners and the CML.

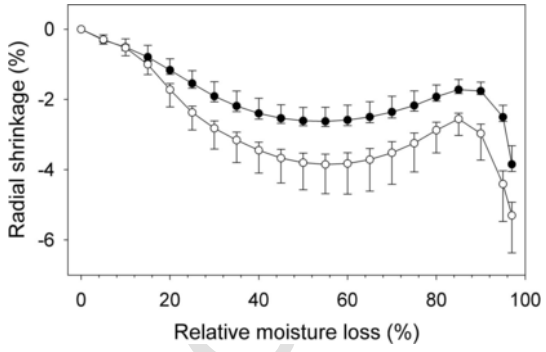

Fig. 3. Courses of the radial shrinkage of Norway spruce sapwood at different stages of relative water loss. Open symbols represent mean values, standard errors and standard deviations for sapwood from a young Norway spruce tree prone to cracking that had a visible lucid band ($n = 8$) and closed symbols "normal" sapwood from a Norway spruce tree with similar age harvested in Ekebo, southern Sweden ($n = 7$).

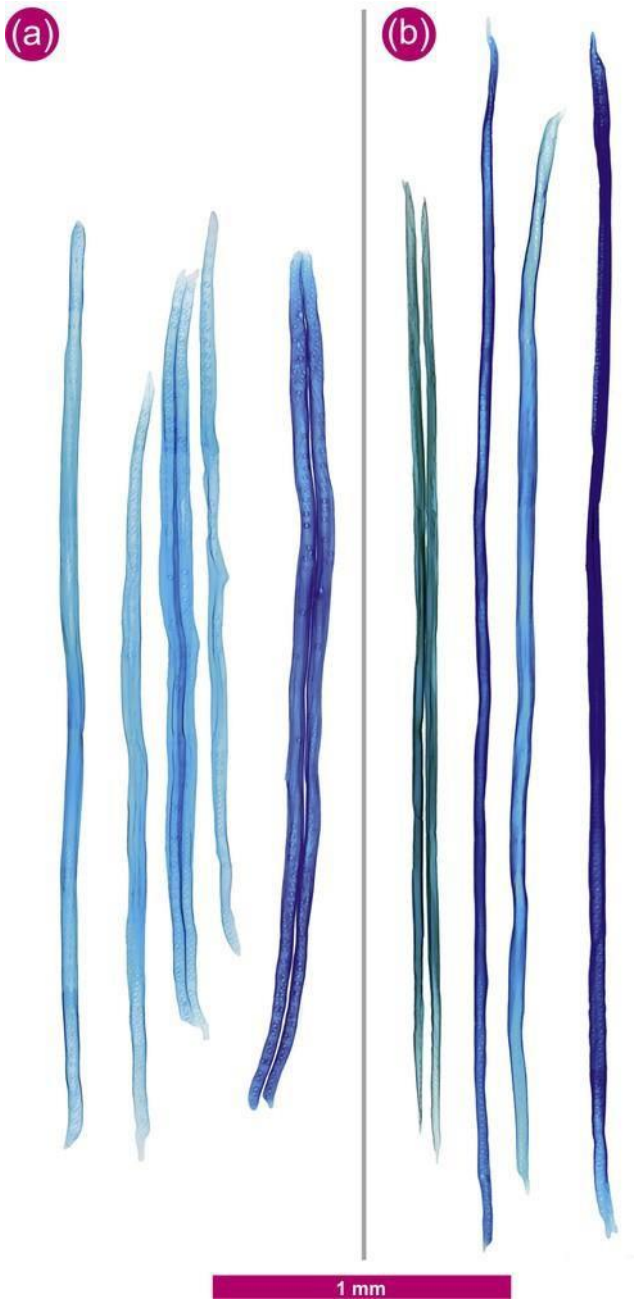

Fig. 4. Macerated tracheids of Norway spruce sapwood from lucid band regions (a) and from normal earlywood (b) from trees harvested in Ekebo, southern Sweden. After maceration, the tracheids were stained with methylene blue and mounted in a resinous embedding medium. The reference bar indicates 1mm.

3.5. Quantitative anatomy: which morphological features are associated with wall collapse?

In five trees from southern Norway, a chronological comparison of anatomical features between trees that showed signs of cell wall collapse and the nearest neighbour that showed no tracheid deformation was performed. Four out of these five trees showed symptoms of top dieback. The aim was to search for anatomical differences between both groups of trees in years with signs of wall collapse (symptomatic years). No significant differences in ring width were found in the years when collapse was observed. Ring width showed however a continuous

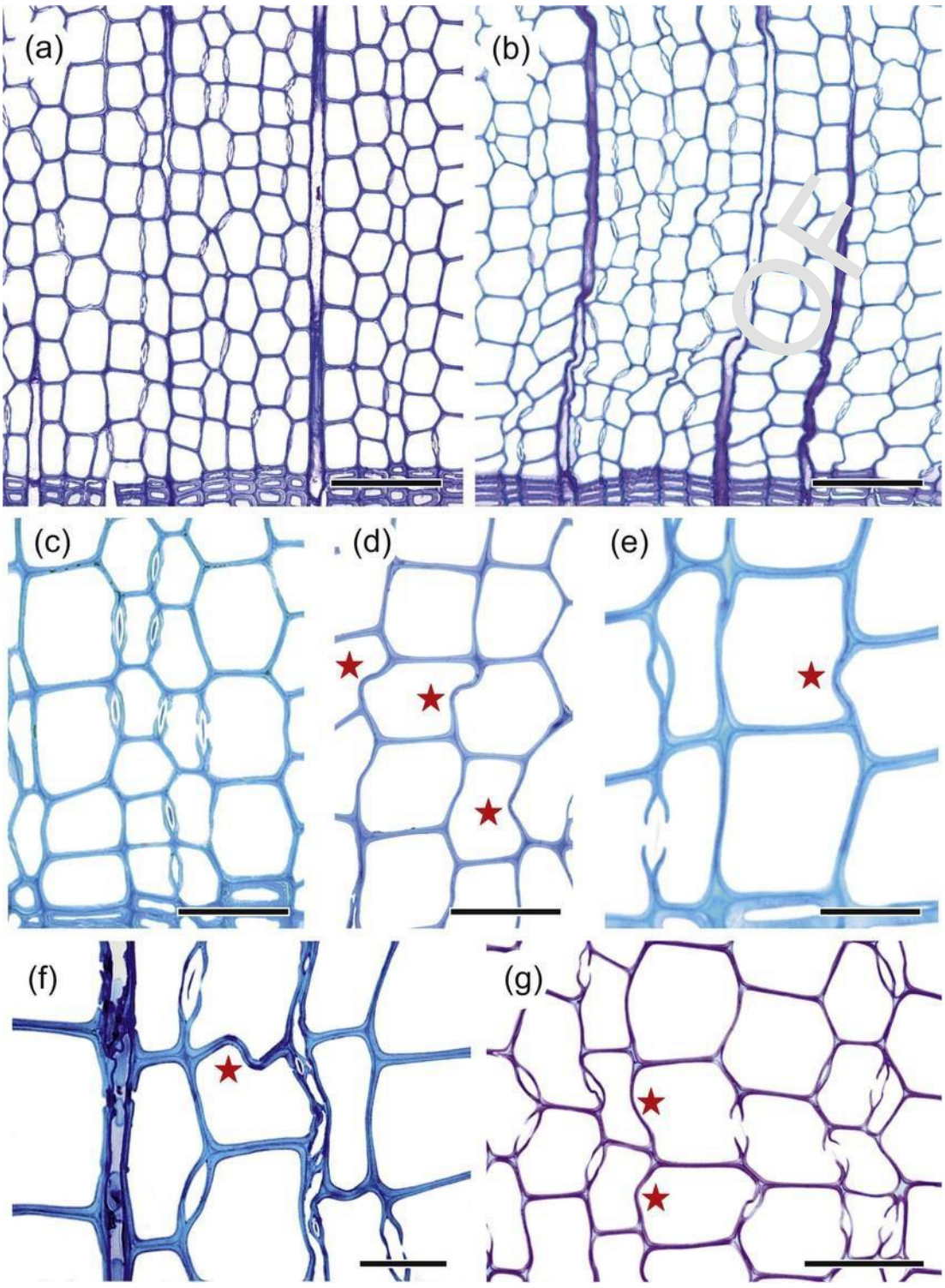

Fig. 5. Normal earlywood (a, c) and earlywood from regions of lucid bands with signs of collapse (b, d–g) of Norway spruce trees harvested in Ekebo, southern Sweden. Deformed tracheid double walls are indicated by stars in images d–g; collapsed walls are not marked in the overview image (b). The reference bar indicates 100 µm in images a and b, 50 µm in images c, d and g, and 25 µm in images e-f. The specimens in images a, b and g were stained with crystal violet, all other specimen with methylene blue.

decrease in trees prone to collapse thereafter (Supplement Fig. 6). Wood density was slightly lower in rings with signs of collapse. In symptomatic years, tangential tracheid lumen were slightly wider in annual rings with collapse; whereas double wall thickness was lower (Supplement Fig. 6). In a next step, the within-ring differences in symptomatic years of the tree pairs were analysed. Wood density was significantly lower in rings with collapse in the middle part of the annual ring (Supplement Fig. 7a). Trees with collapse in symptomatic years showed thinner cell walls (Supplement Fig. 7d) and significantly wider tangential lumen diameters (Supplement Fig. 7e) and lower tangential tracheid wall reinforcement (Supplement Fig. 7f).

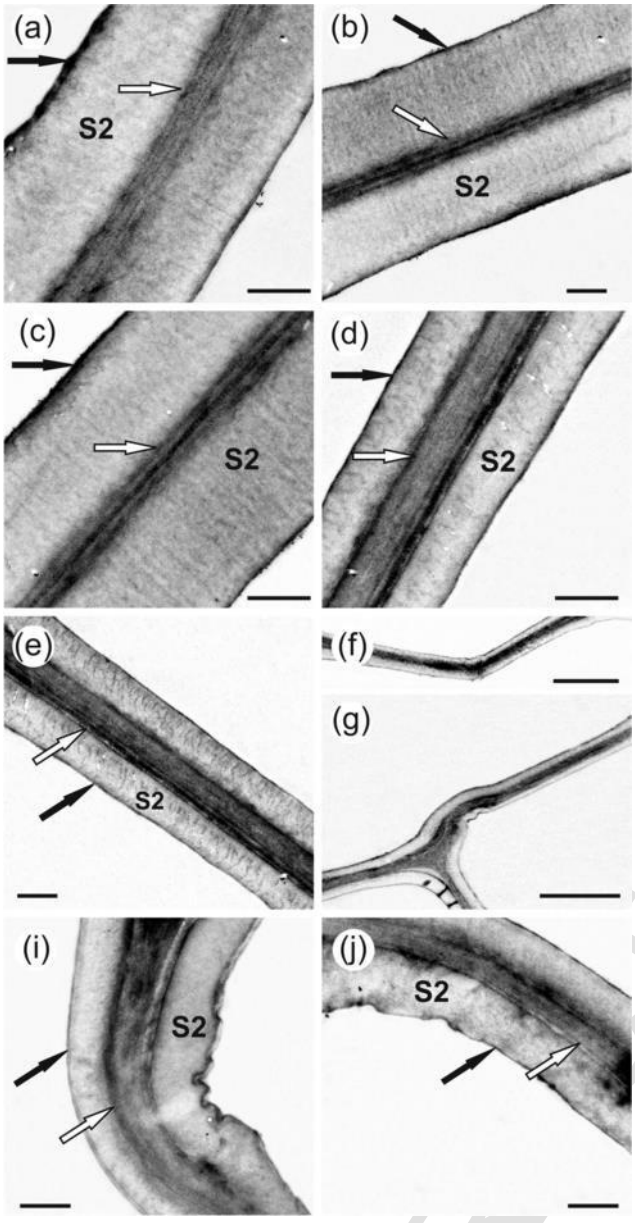

Fig. 6. TEM images of cell walls of tracheids with no signs of collapse (a-c) and with signs of collapse (d-j) of Norway spruce earlywood specimens from Ekebo, southern Sweden. Note that cell walls in the first formed tracheid rows are densely pitted (Fig. 5 g); the layers from the middle lamellae to the S1 in images d–g are therefore slightly thicker. Image (j) gives a good impression on the thickness of these layers in cell wall regions without a bordered pit. The S1 layer is marked by white arrows, the S3 layer by black arrows. Bars in a–e and i, j indicate 1 µm, the bars in f-g indicate 5 µm.

In order to define which cell dimensions are of key importance to avoid mechanical dysfunction, we analysed anatomical traits of the first formed earlywood tracheids of selected rings formed between 2003–2010 in 22 trees from southern Sweden and from 24 trees (Nor- way) where no signs of collapse were found, and compared these re- sults with annual rings of five trees where collapse was present. His- tograms indicated that radial- and tangential lumen diameters showed different distributions in earlywood regions with and without signs of collapse (Fig. 8a and b); mean values were, however, not significantly different (Fig. 9a and b). Radial- and tangential cell wall thickness was significantly lower in regions with collapse (Fig. 9c and d) and the histograms of both traits showed two slightly overlapping clusters (Fig. 8c and d). Histograms of the conduit wall reinforcement traits dif- fered between regions of "normal" tracheids and those in LB regions (Fig. 8e and f), where tracheids in the latter had significantly lower theoretical safety against implosion (Fig. 9e and f). Pit membrane- and aperture diameters used for calculating the theoretical implosion pres- sure differed significantly ($P < 0.01$, n= 20) between normal and col- lapsed tracheids. Membrane- and aperture diameters were larger in collapsed (20.26 ± 0.52 µm, 5.90 ± 0.13 µm) than in normal (18.35 ± 0.40 µm, 5.33 ± 0.12 µm) tracheids. The conduit wall reinforcements used to calculate the implosion pressure for the radial cell walls ($(t_r/b_r)^2$) were 0.0193 for normal and 0.0042 for collapsed tracheids (Fig. 9). The theoretical implosion pressure for the radial cell walls would make up only −0.91 MPa for tracheids prone to collapse but −4.16 MPa for normal earlywood tracheids.

Cell walls of "normal"- and LB tracheids differed not only in the overall thickness (Fig. 10a), but also in the widths of their layers. Whereas the thickness of the CML (Fig. 10e) and S1 layer (Fig. 10b) showed no significant differences between "normal" earlywood- and LB tracheids, LB tracheids had much thinner S2 and S3 layers (Fig. 10c and d). Consequently, the fraction of S1 in proportion to the single cell wall thickness was significantly higher in LB tracheids, the S2 fraction, however, was much lower compared to "normal" tracheids (Fig. 10f and h).

3.6. Genetic and site influence on tracheid wall thickness and wall reinforcement in earlywood

In Fig. 11 the wall thickness in the first 10% of an annual ring of six different clones grown on two sites is shown. Walls were always thicker in a given clone grown on the drier site (Vissefjärda) than on the wetter site (Tönnersjöheden). General linear models indicated a significant influence of the site in all wall- and conduit wall reinforcement traits (Table 1). Wall thickness showed the same trend in different clones (Fig. 11), a significant clonal effect was thus found for all traits investigated, however, no significant clone *x* site interaction was detected (Table 1).

3.7. Climate extremes: the final trigger that causes wall collapse?

The occurrence of collapse in annual rings of trees from Norway could not be related to specific climate-related events, because (a) collapse occurred in different years and not always in the first formed earlywood tracheids, (b) no climate extremes were reported for these years (data not shown) and (c) most of the samples were collected by coring; we can thus not exclude some mechanical damage due to squeezing. We concentrated our investigations on the Ekebo site where 86% of all trees (n = 22) produced in 2006 a "false ring" (Supplement Fig. 8), which is a clear indicator for massive drought stress. Moreover, in two of the trees (9.1%) harvested in Ekebo, signs of collapse were found in the earlywood of the 2006 annual ring. These trees were both prone to stem cracking and included a single young tree that had a genetic predisposition but had developed no crack at the time of harvesting. In 2006, the driest summer since the 1960ties was measured in the weather sta- tion close to (8 km) Ekebo, where the trees were harvested (Supplement Fig. 9b). Precipitation of June and July reached much lower values compared to previous and following years. However, August precipitation was quite high compared to previous years (Supplement Fig. 9c).

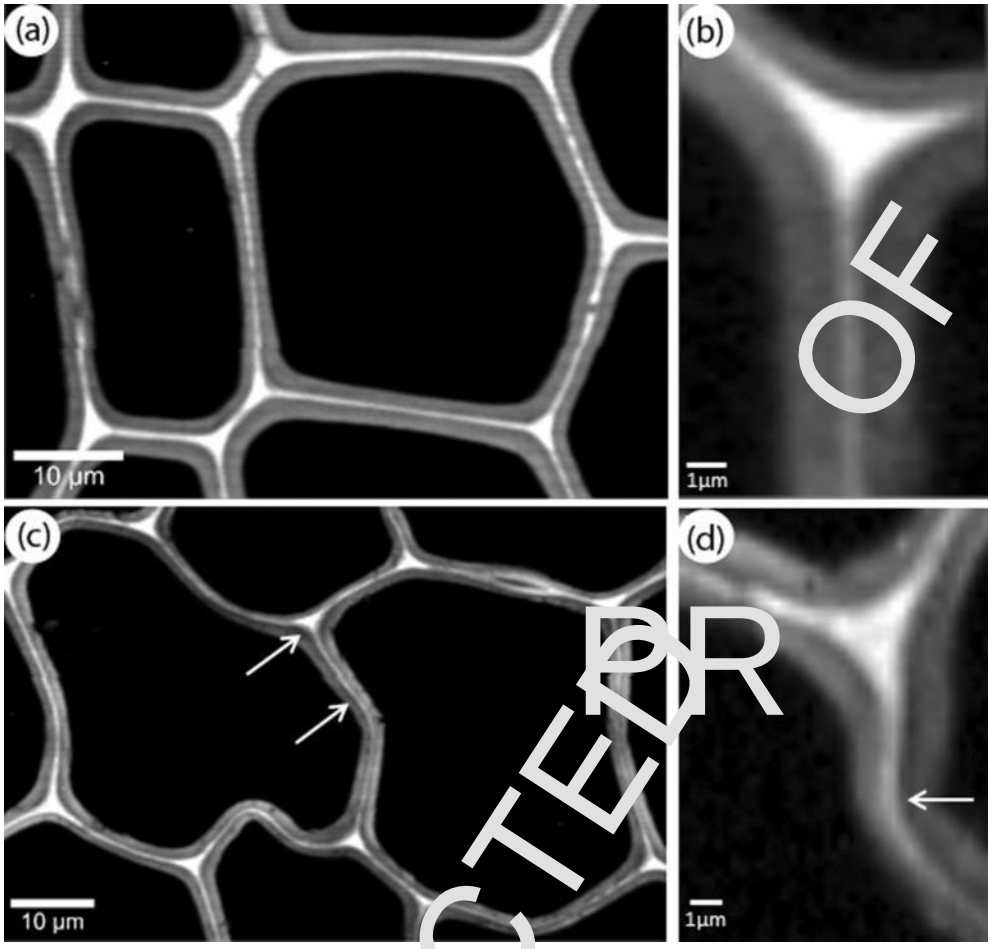

Fig. 7. Lignin distribution visualized by Raman spectroscopy of "normal" earlywood (a, b) earlywood of a lucid band (c, d). Samples came from Norway spruce harvested in Ekebo. Arrows point at regions with inhomogeneous lignin distribution (darker areas) near the compound middle lamellae and cell corners.

4. Discussion

4.1. The occurrence of lucid bands

We decided to introduce the term "lucid bands" (LB) for the lighter (lucid) coloured bands of tracheids which we observed in fresh Norwaysprucesapwood andwith propertiesrelated to collapse on drought, as none of the existing terms "light bands", "light rings", "white rings" nor "blue rings" were adequate. LBs do not represent "blue rings", i.e. bands of non-lignified latewood tracheids indicated by differential staining with safranin/astra-blue (Piermattei et al., 2015), because the observed collapsed tracheids were neither in latewood, nor was a to- tal lack of lignification indicated by Raman spectroscopy (Fig. 7). Instead, safranin/astra-blue red stained cell walls of earlywood tracheids in the LB indicated that they were lignified (Supplement Fig. 5). Further, the lack of lignification in "blue-ring" tracheids is induced by low air temperature during latewood cell wall thickening. LBs are also not "light rings" that are formed in cool summers (Tardif et al., 2011) or "light bands", i.e. extremely thin walled latewood formed in Norway spruce under abnormally low autumn temperatures observed for instance in 1912 after a volcano eruption (Gindl and Grabner, 2000). "White rings" are supposed to be associated with a lower carbohydrate availability in the early growing season of the subsequent year after e.g. defoliation by insects or crown damage due to extreme frost events (Waito et al., 2013). They have an (overall) lighter colour than adja - cent rings, but – contrary to LBs – retain their lighter colour when dried. Finally, the light colour of LBs can only be observed in freshly sampled, non-dried sapwood.

When held against a light source (picture not shown), LB regions appeared somehow less translucent. This loss in translucence is observed when wood lost its function of sap conductance (Světlik et al., 2013). Flow experiments with a staining solution (Hietz et al., 2008) on fully saturated specimens proofed that sap was not transported through the LB regions (Fig. 2). Moreover, light microscopy observations of freshly embedded sapwood (Mayr et al., 2014) indicated that many pits were already aspirated in the regions of the LB (Supplement Fig. 4). The healthy young tree in Ekebo (southern Sweden) with LB was harvested in the early summer season 2008; thus the annual ring 2006 should have been still conductive, if we consider that Norway spruce uses at least ten annual rings for conducting sap (Bertaud and Holmbom, 2004). Regions of LB might have a lighter colour than the later formed sapwood and the sapwood of the previous growth ring because the LB tracheids were filled with air rather than with water. We suggest that LBs have not been observed and/or described so far, because for dendrochronological or dendroecological research it is quite common that specimens are dried immediately after sampling (after wood coring for instance).

4.2. Cell wall collapse in earlywood of Norway spruce is possible

We found irreversible, plastic deformation, in tracheids of Norway spruce wood from field grown trees in southern Scandinavia (Fig. 5,

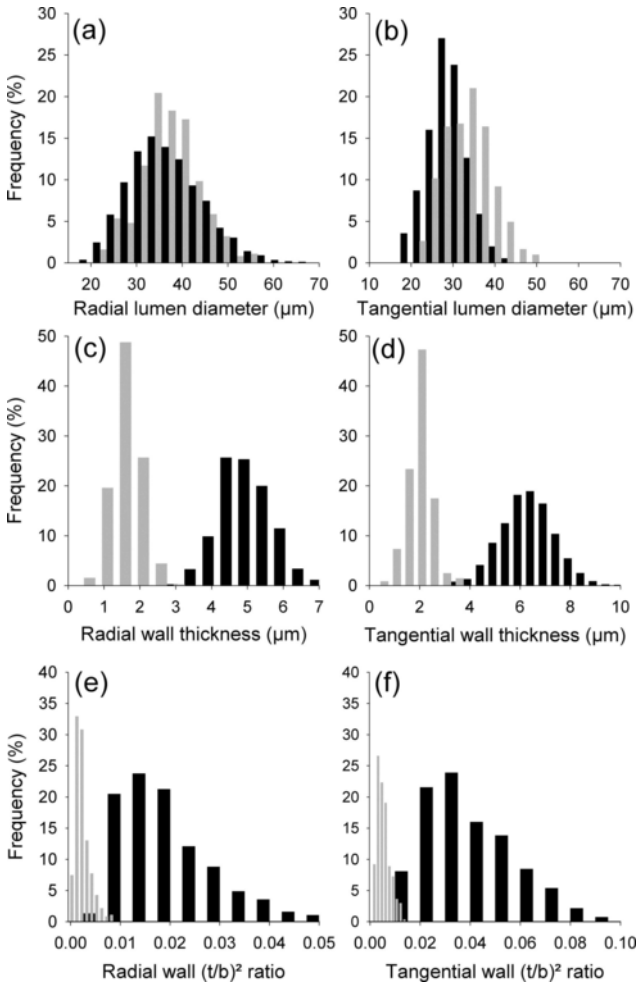

Fig. 8. Histograms of radial (a) and tangential (b) lumen diameter, radial (c) and tangential (d) cell wall thickness and $(t/b)^2$ derived from radial lumen diameter/radial wall (e) and tangential lumen diameter/tangential wall (f) of the first formed earlywood tracheids of selected rings formed between 2003–2010 in 22 trees from southern Sweden and in 24 trees from southern Norway where no signs of collapse were found (black bars) compared to annual rings of five trees where collapse was present (grey bars). An overview of the dataset for the histograms is given in Supplement Table 2.

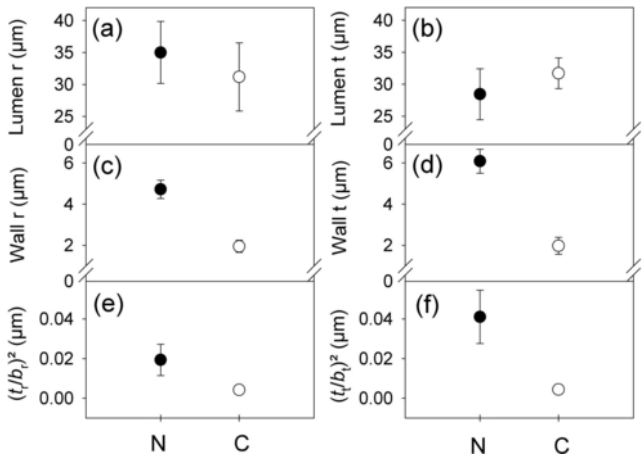

Fig. 9. Anatomic characteristics of tracheids from earlywood formed between 2003 and 2006 of 22 trees from Ekebo (southern Sweden) and from earlywood produced in 2010 of 24 trees from southern Norway for earlywood with hydraulic dysfunction ("collapse"= Y; annual rings with collapse of 2 trees from Sweden and of 3 trees from Norway) and earlywood with no such signs ("collapse" = N; annual rings with no signs of collapse of 22 trees from Sweden and of 24 trees from Norway). Samples from the Swedish trees were taken at breast height, those from the Norwegian trees in the living crown. Tree mean values and standard deviations of anatomical features comprise radial- (a) and tangential lumen diameter (b), radial- (c) and tangential double wall thickness (d) and the conduit wall reinforcement in the radial direction (e) and in the tangential direction (f).

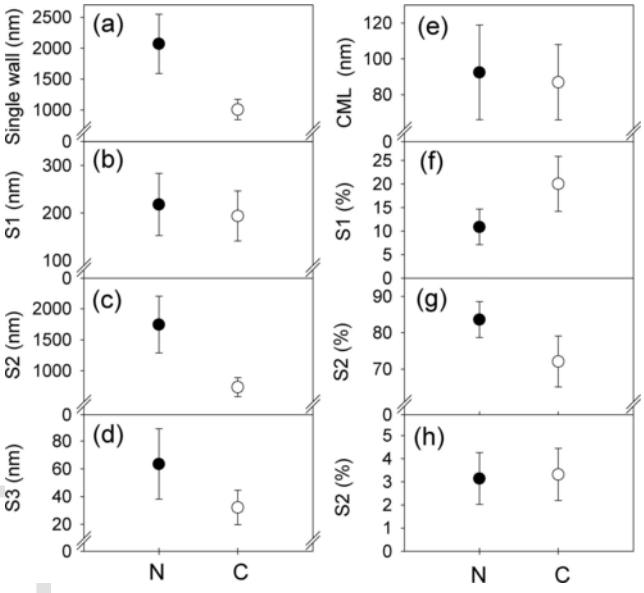

Fig. 10. Thickness of single cell walls (a) and wall layers (compound middle lamellae (e), S1 (b), S2 (c) and S3 (d)) as well as percentages of S layers of the wall related to cell wall thickness of tracheids (f-h) from earlywood of trees from Ekebo (southern Sweden), without ("collapse" = N, n= 2 trees) and with hydraulic dysfunction ("collapse" = C, n= 2 trees) of annual rings formed between 2003 and 2010. Each mean value and the standard deviation was calculated from measurements on 40 tracheids (i.e. 20 double cell walls). Significant differences at the 0.1% level (at least) are indicated by different letters.

Supplement Fig. 4). Observations of such abnormal deformations have been reported for other conifer species either under the impact of artificially induced drought (Glerum, 1970; Barnett, 1976) or in lum- ber from trees growing at sites with periodic severe drought conditions (Donaldson, 2002). Extreme, artificially induced, drought during cambial growth can result in tracheids that totally lack lignin in the secondary wall, which consequently leads to cell wall collapse. In that case, collapse occurs prior to the completion of wall differentiation, since lignification lags behind cellulose production in the cell walls of tracheids (Barnett, 1976; Gricar et al., 2006). Donaldson (2002) found tracheids with concentric layers of abnormal lignification in the secondary cell wall and a reduced lignification of the middle lamella in *Pinus radiata* trees grown under severe water stress. According to the results obtained by Raman imaging, "normal" tracheids showed a straight CML with high lignin content, whereas the CML in the LB tracheids looked thinner and less homogenous. In addition, lignin distribution in the S1 and S2 layers was less homogenous than in "normal" early- wood tracheids (Fig. 7). However, only a severe reduction of lignifica- tion would result in collapsed tracheids, which implies that even par- tial lignification of the secondary wall is sufficient to allow water conduction when it is combined with an appropriate cell wall thickness and a well-developed S3 layer. The S3 layer was thinner, but well developed in tracheids with signs of collapse (Fig. 6i) when compared to findings of normally developed Norway spruce earlywood tracheids (Singh and Daniel, 2001). Donaldson (2002) supposed that reduced lignifications of the middle lamellae in the radial cell walls could af- fect bordered pit functioning due to leakage of water into extracellu- lar spaces that may result in pit aspiration. Also Glerum (1970) re- ports that wall thickness rather than a lack of lignification causes tra- cheid collapse in *Picea glauca* seedlings under severe drought. "Drought

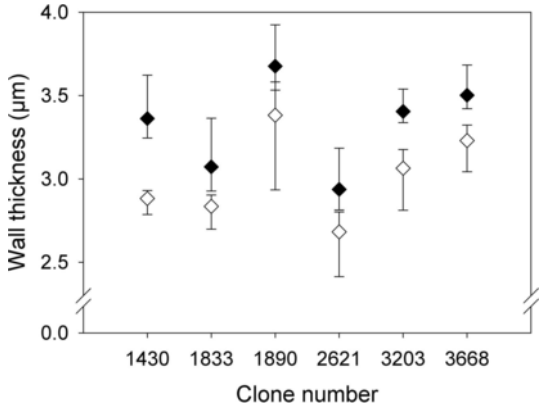

Fig. 11. Double wall thickness assessed by SilviScan technology in the first 10% of annual rings 17–19 of six different Norway spruce clones harvested in Tönnersjöheden (empty symbols, n trees = 27), and Vissefjärda (filled symbols, n trees = 25). Vissefjärda site was drier than the Tönnersjöheden site. The error bars indicate both the standard error and the standard deviation for each mean value. Detailed information on the sites can be found in Rosner et al. (2008).

rings" developed as bands of tracheids that had lignified but thinner cell walls and a reduced radial diameter with signs of collapse. Contrary to the LBs described in our study, the tangential walls in *P. glauca* were extremely deformed, whereas the radial walls remained merely "in line".

The thickness of the S2 layer in tracheids without collapse corresponded to data reviewed in Bergander and Salmén (2000) and Brändström (2001) for Norway spruce earlywood. We found no significant difference in thickness of S1 between normal and collapsed tracheids, but the S2 layer was more than twice as thick in normal tracheids than in tracheids with signs of collapse. The S2 proportion was higher in normal tracheids (82.7%) than in collapsed tracheids (72.10%). Both values lay in the normal range reported for the S2 per- centage based on literature (Brändström, 2001), whereas the proportion of the S1 was much higher in collapsed tracheids (20.0%) than in nor- mal tracheids (11.5%). The mean S1 percentage found in collapsed tracheids was high but did not exceed the maximum of 21.8% reviewed in literature (Brändström, 2001). Overall, radial and tangential walls of tracheids with signs of collapse were much thinner than in mechanically well designed earlywood tracheids, whereas the radial and tangential lumen diameter showed no significant differences (Fig. 8). Histograms of double wall thickness showed two clusters that had a slight over- lap at 3 µm and 4 µm for radial and tangential walls, respectively (Fig. 8). Trees prone to wall collapse operated at the limit concerning their biomechanical design. The conduit wall reinforcement calculated from radial lumen diameters was 0.02 in "normal" earlywood tracheids, but only 0.004 in tracheids with wall collapse. When $(t/b)^2$ was calculated for tangential diameters, even ten times lower values were found in earlywood tracheids prone to collapse than in "normal" tracheids (Fig. 9). The $(t/b)^2$ values given in Fig. 9 describe only the weakest, low den- sity, parts of earlywood from annual rings of the main trunk. Therefore, even the conduit wall reinforcement for "normal" tracheids only reach the minimum values of data published so far for whole earlywood re- gions (Rosner et al., 2016a) and are much lower than in branch early- wood of different conifer species (Bouche et al., 2014). The $(t/b)^2$ cal- culated from tangential lumen diameter showed significant differences when within annual ring variations of tree pairs with and without wall collapse were compared, whereas the $(t/b)^2$ calculated from radial diam- eters did not (Supplement Fig. 7). This is in accordance with our recent findings where $(t/b)^2$ calculated from tangential lumen diameters had a higher predictive quality for hydraulic safety (P_{50}) than that calculated from radial lumen diameters (Rosner et al., 2016b).

Table 1
General linear models (fixed factors: clone and site) for double wall thickness from tracheids located in the first 10% and 25% of the annual ring and of earlywood (EW) tracheids. Samples were taken at breast height. The wetter site is Tönnersjöheden (T), the drier site Vissefjärda (V). SQ= sum of squares; and SE = standard error.

Trait	Site	Mean (SE)	Source clone			Source site			Source clone × site		
			SQ	F	*P* > *F*	SQ	F	*P* > *F*	SQ	F	*P* > *F*
Wall thickness 10% of ring width (µm)	T	3.01 (0.07)	2.90	9.15	0.000	1.25	19.46	0.000	0.08	0.26	0.933
	V	3.32 (0.06)									
Wall thickness 25% of ring width (µm)	T	3.07 (0.06)	2.85	10.93	0.000	0.97	18.69	0.000	0.11	0.43	0.822
	V	3.34 (0.07)									
Wall thickness of EW tracheids (µm)	T	3.38 (0.06)	2.38	8.55	0.000	0.73	13.18	0.001	0.19	0.68	0.638
	V	3.62 (0.06)									
$(t/b_i)^2$ of 10% of ring width	T	0.015 (0.001)	0.00024	3.46	0.011	0.00013	9.59	0.004	0.00002	0.25	0.938
	V	0.018 (0.001)									
$(t/b_i)^2$ of 25% of ring width	T	0.015 (0.001)	0.00025	3.98	0.005	0.00012	9.43	0.004	0.00002	0.29	0.914
	V	0.018 (0.001)									
$(t/b_i)^2$ of EW tracheids	T	0.020 (0.001)	0.00024	2.86	0.027	0.00015	8.71	0.005	0.00001	0.16	0.977
	V	0.023 (0.001)									

4.3. Catastrophic mechanical and hydraulic xylem dysfunction in 2006 in trees from Sweden

In summer 2006, extremely low precipitation in June and July was recorded in the region of the Swedish study trees. This region is close to the city of Lund in southern Sweden, where the highest mean July summer temperature was measured in 2006 since records started in 1859 (SMHI). The influence of climate (temperature and precipitation) on annual variability in the mean cell wall thickness of Norway spruce tracheids is rather weak (Rosner et al., 2016b). Precipitation in September of the previous growing season and in May/June can influence lumen diameters positively (Gričar et al., 2015) and consequently $(t/b)^2$ negatively (Rosner et al., 2016b). It is assumed that by the end of May/beginning of June cell division and elongation of the first earlywood cell rows has already taken place. In the southern boreal zone about 10% of the radial increment develops between late May to early June, half of the annual ring is formed by the first week of July, and 90% of the annual ring is already completed in late July/beginning of August (Mäkinen et al., 2003; Henttonen et al., 2009; Jyske et al., 2014). In 2006, May precipitation was normal for southern Sweden (Supplement Fig. 9a). It is suggested that the initial stages of cell differentiation, i.e. division and elongation, in the first tangential bands of tracheids took place under sufficient moisture supply. Wall thickening was initially undergoing a normal development, but severe drought stress is likely to have affected the final stages of cell differentiation, especially the thickening and lignification of the secondary wall. Under the impact of gradually increasing drought stress due to ongoing lack of precip- itation in June and July, trees invested in producing a distinct false ring rather than in the proper design of the first formed earlywood tra- cheids (Supplement Fig. 8). Since August was relatively wet, cell divi- sion started again at that time. It is likely that in August the collapse in the LB regions had occurred already and the question is if the tra- cheids were capable of conducting water before they were mechanically deformed. The theoretical implosion pressure for the radial cell walls was less negative, −0.91 MPa, for tracheids prone to collapse and much lower, −4.16 MPa, for "normal" earlywood tracheids. In young ma- ture trunkwood of Norway spruce trees grown in southern Sweden P_{50} can range between −3.06 MPa and −1.98 MPa (−2.41 ± 0.03 MPa) and P_{88} between −3.99 MPa and −2.41 MPa (−2.41 ± 0.04 MPa) (Rosner et al., 2014). Mayr et al. (2006) report minimum water potentials of −4.34 ± 0.07 MPa in branches of Norway spruce grown at the alpine timberline. Branches have much higher safety factors than the main trunk or roots (Domec et al., 2009) since much more negative water potentials can develop in the tracheids that are closer to the tree top. It is not very likely that the water potential in the sapwood of the main trunk of a living tree reaches such low water potentials as reported for branches by Mayr et al. (2006); "normal" Norway spruce sapwood in our study had thus a sufficient hydraulic safety (−4.16 MPa). Under the impact of drought stress, the pre-dawn water potential of twigs can drop down to −2.5 MPa (Netherer et al., 2015), which implies that during the day less than −1 MPa could be easily reached in the main trunk. In the LB sapwood regions, water potentials below −0.91 MPa would (theoretically) result in wall collapse. We suggest that cell wall collapse of tracheids with an insufficient hydraulic design can be induced by extreme summer drought, as observed 2006 in southern Sweden. It is also suggested that LB tracheids were functional only for a very short period after their formation.

4.4. Low density earlywood is prone to internal cracking under the impact of severe drought

We suppose that radial cracks can easily develop within lucid bands, and spread in an axial and radial direction towards the bark. The wounds in the bark produced by the cracks are sources for fungal in- fection; the tree has to invest carbohydrates for wound reaction and defence (Morris et al., 2016). Moreover, the tree loses a lot of its sap- wood area, if we assume that – under normal conditions – at least the last ten annual rings are capable of conducting sap (Bertaud and Holmbom, 2004). Sapwood from trees that are prone to internal crack- ing showed extreme changes in shrinkage above 30% moisture content when compared to "normal" sapwood (Rosner et al., 2009). Such dif- ferential swelling/shrinking processes induced by high tension forces of free water in capillaries and conduits could lead to crack formation. Within-ring crack formation in living Norway spruce trees due to "*an imbalance between water loss and water replenishment during the dormant season*" has been observed by Cherubini et al. (1997). In the ring where a crack was formed, the earlywood tracheids show wall collapse and the rays have the typical wavy structure as observed in our specimens (Fig. 5b, Supplement Fig. 3). Similar observations were made by Lutz (1952) in *Picea glauca*, where extremely high tensions that develop in water filled tracheids cause internal cracking. The crack is often not produced in the year when the low density wood was developed, but one or two years later under severe summer drought (Grabner et al., 2006). Cracks along the trunk are a not so rarely observed phenom- enon that can occur especially in young and fast growing (annual ra- dial increment >8 mm) Norway spruce trees at the age between 20 and 40 years (Caspari and Sachsse, 1990; Persson, 1994; Ferenczy and Tomiczek, 1996). As such, Persson (1994) warned against the cultiva- tion of fast growing eastern European Norway spruce provenances in southern Scandinavia, because low wood density is the major cause of economic losses, rather than the cracking itself. Even if cracks do not occur because of the lack of a dry period, the timber may be not suitable for structural purposes and may contain too little dry matter to be mar- ketable as raw material for chemical pulp. Moreover, even if the inter- nal cracks do not occur out in the field, they may develop in the lumber during industrial kiln drying (Putoczki et al., 2007).

5. Conclusions

Cell wall collapse was not present in all trees with stem cracks investigated, but based on our dataset we conclude that conifer wood is often lacking a resistance against implosion or cell wall collapse. Tracheids with radial double cell walls much thinner than 3 µm (mean of 2 µm) and a mean $(t_r/b_r)^2$ of 0.004 are prone to cell wall collapse. As hypothesized, we found that the critical factor is not the lumen diameter, which showed similar values in both "normal" and collapsed tracheids, but the cell wall thickness that has a quite high heritability in Norway spruce (Chen et al., 2016). Cell wall thickness has a strong influence on wood density and wood density is genetically inversely related to growth in Norway spruce (Hannrup et al., 2004; Chen et al., 2014). Provenances or individuals that produce earlywood with extremely thin cell walls can develop cell wall collapse and internal cracks under the impact of extreme dry summer spells, which are likely to become more frequent in the near future (IPCC, 2013). We propose inspection for lucid bands (LBs) as a new diagnostic tool for risk of cell wall collapse and the initiation of cracks. To detect LBs, field diagnosis is necessary because once the sapwood has dried, the lucid bands will have the same colour as the earlywood of adjacent annual rings. LBs have a lighter colour than the later formed sapwood and the sapwood of the previous growth ring because the tracheids in these zones are

filled with air or water vapour. In addition, in LBs, the bordered pits are merely aspirated and the capacity to conduct water has been lost irreversibly. This phenomenon has not been described so far and we suggest similar studies on other conifer species in order to face the threats to hydraulic functioning of trees under extreme summer drought. The detection of genotypes with LBs could be useful for an early selection of individuals that are prone to stem cracks under the impact of severe summer drought, and also for early downgrading of logs prone to cracking during kiln drying.

Acknowledgements

The work of N. Gierlinger was funded by the Austrian Science Fund (FWF): START Project [Y-728-B16]. Sampling was financed by the Norwegian Research Council (project "Dieback in Norway spruce", No. 199403), by the Norwegian Forest Owners' Research Fund "Skogtiltaksfondet", and six regional funds in Norway (Fylkesmannen).We thank Rainer Hentschel and Saskia Luss for assistance in the field and in the laboratory. We thank two anonymous reviewers for their input to a former version of the manuscript and Dr. Laclau for fast proceeding of the reviewing process.

Author contributions

BK was responsible for site and tree selection on the Swedish study sites; LD and SS were responsible for the project design and project management of the Norwegian study sites; JS, KA, IB, LD and SR contributed to field work, tree selection and sample preparation. SR conducted hydraulic- and shrinkage measurements and descriptive and quantitative anatomy; NG carried out Raman imaging and data interpretation; RE and S-OL were responsible for SilviScan measurements; BK provided climate raw data. SR analysed the whole dataset; all authors contributed to the interpretation of the results; SR wrote a first draft of the manu- script; SJ, NG and MK revised the first draft, all authors revised the sec- ond draft by rewriting, discussion and commenting.

Conflict of interest

The authors declare that they have no conflicts of interest.

Appendix A. Supplementary material

Supplementary data associated with this article can be found, in the online version, athttps://doi.org/10.1016/j.foreco.2017.11.051.

References

Allen, C.D., Breshears, D.D., McDowell, N.G., 2015. On underestimation of global vulnerability to tree mortality and forest die-off from hotter drought in the Anthropocene. Ecosphere 6 (8), 1–55. https://doi.org/10.1890/ES15-00203.1, art129.

Andreassen, K., Solberg, S., Tveito, O.E., Lystad, S.L., 2006. Regional differences in climatic responses of Norway spruce (Picea abies L. Karst) growth in Norway. For. Ecol. Manage. 222, 211–221. https://doi.org/10.1016/j.foreco.2005.10.029.

Barnett, J.R., 1976. Rings of collapsed cells in Pinus radiata stemwood from lysime- tergrown trees subjected to drought. N. Z. J. For. Sci. 6 (2), 461–465.

Bergander, A., Salmén, L., 2000. Variations in transverse fibre wall properties: relations between elastic properties and structure. Holzforschung 54 (6), 654–660. https://doi.org/10.1515/HF.2000.110.

Bertaud, F., Holmbom, B., 2004. Chemical composition of earlywood and latewood in Norway spruce heartwood, sapwood and transition zone wood. Wood Sci. Technol. 38, 245–256. https://doi.org/10.1007/s00226-004-0241-9.

Bouche, P.S., Larter, M., Domec, J.-C., Burlett, R., Gasson, P., Jansen, S., Delzon, S., 2014. A broad survey of hydraulic and mechanical safety in the xylem of conifers. J. Exp. Bot. 65, 4419–4431. https://doi.org/10.1093/jxb/eru218.

Brändström, J., 2001. Micro- and ultrastructural aspects of Norway spruce tracheids: A review. IAWA J. 22 (4), 333–353.https://doi.org/10.1163/22941932-90000381.

Brodribb, T.J., Holbrook, N.M., 2005. Water stress deforms tracheids peripheral to the leaf vein of a tropical conifer. Plant Physiol. 137, 1139–1146. https://doi.org/10.1104/pp.104.058156.

Carpita, N.C., McCann, M.C., 2015. Characterizing visible and invisible cell wall mutant phenotypes. J. Exp. Bot. 66, 4145–4163. https://doi.org/10.1093/jxb/erv090.

Caudullo, G., Tinner, W., de Rigo, D., 2016. Picea abies in Europe: distribution, habitat, usage and threats. In: San-Miguel-Ayanz, J., de Rigo, D., Caudullo, G., Houston Durrant, T., Mauri, A. (Eds.), European Atlas of Forest Tree Species, pp. e012300+. Publ. Off. EU, Luxembourg. https://w3id.org/mtv/FISE-Comm/v01/e012300

Chen, Z.-Q., Gil, M.R.G., Karlsson, B., Lundqvist, S.-O., Olsson, L., Wu, H.X., 2014. Inheritance of growth and solid wood quality traits in a large Norway spruce population tested at two locations in southern Sweden. Tree Genet. Genomes 10, 1291–1303. https://doi.org/10.1007/s11295-014-0761-x.

Chen, Z.-Q., Karlsson, B., Mörling, T., Olsson, L., Mellerowicz, E.J., Wu, H.X., Lundqvist, S.-O., García Gil, M.R., 2016. Genetic analysis of fiber dimensions and their correlation with stem diameter and solid-wood properties in Norway spruce. Tree Genet. Genomes 12, 123. https://doi.org/10.1007/s11295-016-1065-0.

Cherubini, P., Schweingruber, F.H., Forster, T., 1997. Morphology and ecological significance of intra-annual radial cracks in living conifers. Trees 11, 216–222. https://doi.org/10.1007/s004680050078.

Choat, B., Jansen, S., Brodribb, T.J., Cochard, H., Delzon, S., Bhaskar, R., Bucci, S.J., Feild, T.S., Gleason, S.M., Hacke, U.G., Jacobsen, A.L., Lens, F., Maherali, H., Martínez-Vilalta, J., Mayr, S., Mencuccini, M., Mitchell, P.J., Nardini, A., Pitterman, J., Pratt, R.B., Sperry, J.S., Westoby, M., Wright, I.J., Zanne, A.E., 2012. Global convergence in the vulnerability of forests to drought. Nature 491, 752–755. https://doi.org/10.1038/nature11688.

Cochard, H., Froux, F., Mayr, S., Coutand, C., 2004. Xylem wall collapse in water-stressed pine needles. Plant Physiol. 134, 401–408.https://doi.org/10.1104/pp.103.028357.

Domec, J.-C., Warren, J.M., Meinzer, F.C., Lachenbruch, B., 2009. Safety for xylem failure by implosion and air-seeding within roots, trunks and branches of young and old conifer trees. IAWA J. 30 (2), 101–120. https://doi.org/10.1163/ 22941932-90000207.

Donaldson, L.A., 2002. Abnormal lignin distribution in wood from severely drought stressed Pinus radiata trees. IAWA J. 23, 161–178. https://doi.org/10.1163/22941932-90000295.

Downes, G., Turvey, N.D., 1990. Does water-stress lead to formation of traumatic tissue and tracheid collapse in poorly lignified Pinus radiata?. For. Ecol. Manage. 30, 139–145. https://doi.org/10.1016/0378-1127(90)90132-U.

Evans, R., 1994. Rapid measurement of the transverse dimensions of tracheids in radial wood sections from Pinus radiata. Holzforschung 48, 168–172. https://doi.org/10.1515/hfsg.1994.48.2.168.

Evans, R., 1999. A variance approach to the X-ray diffractometric estimation of microfibril angle in wood. Appita J. 52 (4), 283–289.

Caspari, C.-O., Sachsse, H., 1990. Rißschäden an Fichte - Verbreitung, Schadbild, Ursache, Auswirkungen. Forst und Holz 45, 685–688.

Ferenczy, J., Tomiczek, C., 1996. Stammrisse in wüchsigen Fichtenbeständen. Forstschutz aktuell 17 (18), 25.

Gauthier, S., Bernier, P., Kuuluvainen, T., Shvidenko, A.Z., Schepaschenko, D.G., 2015. Boreal forest health and global change. Science 349, 819–822. https://doi.org/10.1126/science.aaa9092.

Gierlinger, N., Keplinger, T., Harrington, M., 2012. Imaging of plant cell walls by confocal Raman microscopy. Nat. Protoc. 7 (9), 1694–1708. https://doi.org/10.1038/nprot.2012.092.

Gindl, W., Grabner, M., 2000. Characteristics of spruce (Picea abies (L.) Karst) latewood formed under abnormally low temperatures. Holzforschung 54, 9–11. https://doi.org/10.1515/HF.2000.002.

Glerum, C., 1970. Drought ring formation in conifers. For. Sci. 16, 246–248.

Grabner, M., Cherubini, P., Rozenberg, P., Hannrup, B., 2006. Summer droughtandlow earlywood density induce intra-annual radial cracks in conifers. Scand. J. For. Res. 21, 151–157. https://doi.org/10.1080/02827580600642100.

Gričar, J., Prislan, P., deLuis, M., Gryc, V., Hacurová, J., Vavrcík, H., Čufar, K., 2015. Plasticity in variation of xylem and phloem cell characteristics of Norway spruce under different local conditions. Front. Plant Sci. 6, 730. https://doi.org/10.3389/fpls.2015.00730.

Gricar, J., Zupancic, M., Cufar, K., Koch, G., Schmitt, U., Oven, P., 2006. Effect of local heating and cooling on cambial activity and cell differentiation in the stem of norway spruce (Picea abies). Ann. Bot. 97, 943–951.https://doi.org/10.1093/aob/mcl050.

Hacke, U.G., Jansen, S., 2009. Embolism resistance of three boreal conifer species varies with pit structure. New Phytol. 182, 675–686. https://doi.org/10.1111/j.1469-8137.2009.02783.x.

Hacke, U.G., Sperry, J.S., Pittermann, J., 2004. Analysis of circular bordered pit function II. Gymnosperm tracheids with torus-margo pit membranes. Am. J. Bot. 91, 386–400. https://doi.org/10.3732/ajb.91.3.386.

Hacke, U.G., Sperry, J.S., Pockman, W.T., Davis, S.D., McCulloh, K., 2001.Trendsinwood density and structure are linked to prevention of xylem implosion by negative pressure. Oecologia 126, 457–461. https://doi.org/10.1007/s004420100628.

Hannrup, B., Cahalan, C., Chantre, G., Grabner, M., Karlsson, B., Le Bayon, I., Müller, U., Pereira, H., Rodrigues, J.C., Rosner, S., Rozenberg, P., Wilhelmsson, L., Wimmer, R., 2004. Genetic parameters of growth and wood quality traits in Picea abies. Scand. J. For. Res. 19, 14–29. https://doi.org/10.1080/02827580310019536.

Hentschel, R., Rosner, S., Kayler, Z.E., Andreassen, K., Børja, I., Solberg, S., Tveito, O.E., Priesack, E., Gessler, A., 2014. Norway spruce physiological and anatomical predis -

position to dieback. For. Ecol. Manage. 322, 27–36. https://doi.org/10.1016/j.foreco.2014.03.007.
Henttonen, H.M., Mäkinen, H., Nöjd, P., 2009. Seasonal dynamics of the radial increment of Scotspine and Norway spruce in the southern andmiddle borealzones in Finland. Can. J. For. Res. 39, 606–618. https://doi.org/10.1139/X08-203.
Hereş, A.-M., Camarero, J.J., López, B.C., Martínez-Vilalta, J., 2014. Declining hydraulic performances and low carbon investments in tree rings predate Scots pine drought-induced mortality. Trees 28, 1737–1750. https://doi.org/10.1007/s00468-014-1081-3.
Hietz, P., Rosner, S., Sorz, J., Mayr, S., 2008. Comparison of methods to quantify loss of hydraulic conductivity in Norway spruce. Ann. For. Sci. 65, https://doi.org/10.1051/forest:2008023, 502p7.
IPCC, 2013. Climate change 2013: the physical science basis, in: Stocker, T.F., Qin, D., Plattner, G.-K., Tignor, M., Allen, S.K., Boschung, J., Nauels, A., Xia, Y., Bex, V., Midgley, P.M. (Eds.), Contribution of Working Group I to the Fifth Assessment Report of the Intergovernmental Panel on Climate Change, Cambridge University Press, Cambridge; New York, NY, pp. 1535.
Jeffrey, E.C., 1917. The Anatomy of Woody Plants. University of Chicago Press, IL, 478.
Jyske, T., Mäkinen, H., Kalliokoskin, T., Nöjd, P., 2014. Intra-annual tracheid production of Norway spruce and Scots pine across a latitudinal gradient in Finland. Agric. For. Meteorol. 194, 241–254. https://doi.org/10.1016/j.agrformet.2014.04.015.
Kapeller, S., Dieckmann, U., Schueler, S., 2017. Varying selection differential throughout the climatic range of Norway spruce in Central Europe. Evol. Appl. 10 (1), 25–38. https://doi.org/10.1111/eva.12413.
Kauppi, P.E., Posch, M., Pirinen, P., 2016. Large impacts of climatic warming on growth of boreal forests since 1960. PLoS ONE 9, e111340. https://doi.org/10.1371/journal.pone.0111340.
Kaufmann, I., Schulze-Till, T., Schneider, H.U., Zimmermann, U., Jakob, P., Wegner, L.H., 2009. Functional repair of embolized vessels in maize roots after temporal drought stress, as demonstrated by magnetic resonance imaging. New Phytol. 184, 245–256. https://doi.org/10.1111/j.1469-8137.2009.02919.x.
Kitin, P., Voelker, S.L., Meinzer, F.C., Beekman, H., Strauss, S.H., Lachenbruch, B., 2010. Tyloses and phenolic deposits in xylem vessels impede water transport in low-lignin transgenic poplars: a study by cryo-fluorescence microscopy. Plant Physiol. 154, 887–898. https://doi.org/10.1104/pp.110.156224.
Liese, W., Bauch, J., 1967. On the closure of bordered pits in conifers. Wood Sci. Technol. 1, 1–13.
Lutz, H.J., 1952. Occurrence of clefts in the wood of living white spruce in Alaska. J. For. 50, 99–102.
Mäkinen, H., Nöjd, P., Saranpää, P., 2003. Seasonal changes in stem radius and production of new tracheids in Norway spruce. Tree Physiol. 23, 959–968.
Mayr, S., Cochard, H., 2003. A new method for vulnerability analysis of small xylem areas reveals that compression wood of Norway spruce has lower hydraulic safety than opposite wood. Plant, Cell Environ. 26, 1365–1371. https://doi.org/10.1046/j.0016-8025.2003.01060.x.
Mayr, S., Rothart, B., Dämon, B., 2003. Hydraulic efficiency and safety of leader shoots and twigsin Norwaysprucegrowingatthealpinetimberline. J. Exp.Bot. 54, 2563–2568. https://doi.org/10.1093/jxb/erg272.
Mayr, S., Schmid, P., Laur, J., Rosner, S., Charra-Vaskou, K., Dämon, B., Hacke, U.G., 2014. Uptake of water via branches helps timberline conifers refill embolized xylem in late winter. Plant Physiol. 164, 1731–1740. https://doi.org/10.1104/pp.114.236646.
Mayr, S., Hacke, U., Schmid, P., Schwienbacher, F., Gruber, A., 2006. Frost drought in conifers at the alpine timberline: xylem dysfunction and adaptations. Ecology 87, 3175–3185.
McDowell, N.G., 2011. Update on mechanisms of vegetation mortality. mechanisms linking drought, hydraulics, carbon metabolism, and vegetation mortality. Plant Physiol. 155, 1051–1059. https://doi.org/10.1104/pp.110.170704.
McDowell, N.G., Williams, A.P., Xu, C., Pockman, W.T., Dickman, L.T., Sevanto, S., Pangle, R., Limousin, J., Plaut, J., Mackay, D.S., Ogee, J., Domec, J.C., Allen, C.D., Fisher, R.A., Jiang, X., Muss, J.D., Breshears, D.D., Rauscher, S.A., Koven, C., 2016. Multi-scale predictions of massive conifer mortality due to chronic temperature rise. Nat. Clim. Change 6, 295–300. https://doi.org/10.1038/nclimate2873.
Meinzer, F.C., McCulloh, K.A., 2013. Xylem recovery from drought-induced embolism: where is the hydraulic point of no return?. Tree Physiol. 33, 331–334. https://doi.org/10.1093/treephys/tpt022.
Morris, H., Brodersen, C., Schwarze, F.W.M.R., Jansen, S., 2016. The parenchyma of secondary xylem and its critical role in tree defense against fungal decay in relation to the CODIT model. Front. Plant Sci. 7, 1665. https://doi.org/10.3389/fpls.2016.01665.
Netherer, S., Matthews, B., Katzensteiner, K., Blackwell, E., Henschke, P., Hietz, P., Pennerstorfer, J., Rosner, S., Kikuta, S., Schume, H., Schopf, A., 2015. Do water limiting conditions predispose Norway spruce to bark beetle attack?. New Phytol. 205 (3), 1128–1141. https://doi.org/10.1111/nph.13166.
Persson, A., 1994. Stem cracks in Norway spruce in southern Scandinavia: causes and consequences. Ann. For. Sci. 51, 327.
Piermattei, A., Crivellaro, A., Carrer, M., Urbinati, C., 2015. The “blue ring”: anatomy and formation hypothesis of a new tree-ring anomaly in conifers. Trees 29, 613–620. https://doi.org/10.1007/s00468-014-1107-x.
Putoczki, T.L., Nair, H., Butterfield, B., Jackson, S.L., 2007. Intra-ring checking in Pinus radiata D. Don: the occurrence of cell wall fracture, cell collapse, and lignin distribution. Trees 21, 221–229. https://doi.org/10.1007/s00468-006-0114-y.
Rosner, S., Karlsson, B., Konnerth, J., Hansmann, C., 2009. Shrinkage processes in standard-size Norway spruce wood specimens with different vulnerability to cavitation. Tree Physiol. 29, 1419–1431. https://doi.org/10.1093/treephys/tpp077.
Rosner, S., Klein, A., Wimmer, R., Karlsson, B., 2006. Extraction of features from ultrasound acoustic emissions: a tool to assess the hydraulic vulnerability of Norway spruce trunkwood?. New Phytol. 171, 105–116. https://doi.org/10.1111/j.1469-8137.2006.01736.x.
Rosner, S., Klein, A., Müller, U., Karlsson, B., 2008. Tradeoffs between hydraulic and mechanical stress response of mature Norway spruce trunkwood. Tree Physiol. 28, 1179–1188 http://heronpublishing.com/tree/freetext/28-1179.pdf.
Rosner, S., Luss, S., Světlík, J., Andreassen, K., Børja, I., Dalsgaard, L., Evans, R., Tveito, O.E., Solberg, S., 2016a. Chronology of hydraulic vulnerability in trunk wood of conifer trees with and without symptoms of top dieback. J. Plant Hydraul. JPH-3-e001. https://www6.inra.fr/jph/Articles/2016/JPH-3-e001.
Rosner, S., Světlík, J., Andreassen, K., Børja, I., Dalsgaard, L., Evans, R., Karlsson, B., Tollefsrud, M.M., Solberg, S., 2014. Wood density as a screening trait for drought sensitivity in Norway spruce. Can. J. For. Res. 44, 154–161. https://doi.org/10.1139/ cjfr-2013-0209.
Rosner, S., Světlík, J., Andreassen, K., Børja, I., Dalsgaard, L., Evans, R., Luss, S., Tveito, O.E., Solberg, S., 2016. Novel hydraulic vulnerability proxies for a boreal conifer species reveal that opportunists may have lower survival prospects under extreme climatic events. Front. Plant Sci. 7, 1–14. https://doi.org/10.3389/fpls.2016.00831, Article 831.
Schlyter, P., Stjernquist, I., Bärring, L., Jönsson, A.M., Nilsson, C., 2006. Assessment of the impacts of climate change and weather extremes on boreal forests in northern Europe, focusing on Norway spruce. Clim. Res. 31, 75–84. https://doi.org/10.3354/cr031075.
Seidl, R., Vigl, F., Rössler, G., Neumann, M., Rammer, W., 2017. Assessingtheresilienceof Norway spruce forests through a model-based reanalysis of thinning trials. For. Ecol. Manage. 388, 3–12. https://doi.org/10.1016/j.foreco.2016.11.030.
Schneider, C.A., Rasband, W.S., Eliceiri, K.W., 2012. NIHImageto ImageJ: 25 yearsof image analysis. Nat. Meth. 9 (7), 671–675. https://doi.org/10.1038/nmeth.2089.
Singh, A.P., Daniel, G., 2001. The S2 layer in the tracheid walls of Picea abies wood: inhomogeneity in lignin distribution and cell wall microstructure. Holzforschung 55, 373–378. https://doi.org/10.1515/HF.2001.062.
SMHI (Swedish Meteorological and Hydrological Institute), dataset available at: http://data.smhi.se//met/climate/time_series/month/vov_pdf/ (3 October 2017, date last accessed)
Solberg, S., 2004. Summer drought: a driver for crown condition and mortality of Norway spruce in Norway. For. Pathol. 34, 93–104. https://doi.org/10.1111/j.1439-0329.2004.00351.x.
Spinoni, J., Naumann, G., Vogt, J.V., 2017. Pan-European seasonal trends and recent changes of drought frequency and severity. Global Planet. Change 148, 113–130. https://doi.org/10.1016/j.gloplacha.2016.11.013.
Stinziano, J.R., Hüner, N.P.A., Way, D.A., 2015. Warming delays autumn declines in photosynthetic capacity in a boreal conifer, Norway spruce (Picea abies). Tree Physiol. 35 (12), 1303–1313. https://doi.org/10.1093/treephys/tpv118.
Světlík, J., Børja, I., Rosner, S., Čermák, J., Nadezhdin, V., Nadezhdina, N., 2013. Differential translucence method as a supplement to sap flow measurement in Norway spruces with symptoms of top dieback. Acta Hortic. 991, 285–292. https://doi.org/10.17660/ActaHortic. 2013.991.35.
Tardif, J.C., Girardin, M.P., Conciatori, F., 2011. Light rings as bioindicators of climate change in Interior North America. Global Planet. Change 79, 134–144. https://doi.org/10.1016/j.gloplacha.2011.09.001.
Turner, S.R., Somerville, C.R., 1997. Collapsed xylem phenotype of arabidopsis identifies mutants deficient in cellulose deposition in the secondary cell wall. Plant Cell 9, 689–701. https://doi.org/10.1105/tpc.9.5.689.
Wagner, A., Donaldson, L., Kim, H., Phillips, L., Flint, H., Steward, D., Torr, K., Koch, G., Schmitt, U., Ralph, J., 2009. Suppression of 4-coumarate-CoA ligase in the coniferous gymnosperm Pinus radiata. Plant Physiol. 149, 370–383. https://doi.org/10.1104/pp.108.125765.
Waito, J., Conciatori, F., Tardif, J.C., 2013. Frost rings and white earlywood rings in Picea mariana trees from the boreal plains, Central Canada. IAWA J. 34, 71–87. https://doi.org/10.1163/22941932-00000007.
Wimmer, R., 2002. Wood anatomical features in tree-rings as indicators of environmental change. Dendrochronologia 20, 21–36. https://doi.org/10.1078/1125-7865-00005.
Zhang, Y.-J., Rockwell, F.E., Wheeler, J.K., Holbrook, N.M., 2014. Reversibledeformation of transfusion tracheids in Taxus baccata is associated with a reversible decrease in leaf hydraulic conductance. Plant Physiol. 165, 1557–1565. https://doi.org/10.1104/pp.114.243105.
Zhang, Y.-J., Rockwell, F.E., Graham, A.C., Alexander, T., Holbrook, N.M., 2016. Reversible leaf xylem collapse: a potential 'circuit breaker' against cavitation. Plant Physiol. 172 (4), 2261–2274. https://doi.org/10.1104/pp.16.01191.
Zwieniecki, M.A., Secchi, F., 2015. Threats to xylem hydraulic function of treesunder 'new climate normal' conditions. Plant, Cell Environ. 38, 1713–1724. https://doi.org/10.1111/pce.12412.